HHS Public Access

Author manuscript

Rapid Commun Mass Spectrom. Author manuscript; available in PMC 2015 March 15.

Published in final edited form as:

Rapid Commun Mass Spectrom. 2014 March 15; 28(5): 403–412. doi:10.1002/rcm.6796.

Improved Spatial Resolution of MALDI Imaging of Lipids in the Brain by Alkylated Derivatives of 2,5-Dihydroxybenzoic Acid

D.A. Stoyanovsky[1,2,*], **L.J. Sparvero**[1,2], **A.A. Amoscato**[1,2], **R.R. He**[1,2,5], **S. Watkins**[3], **B.R. Pitt**[1], **H. Bayir**[1,2,4,*], and **V.E. Kagan**[1,2,*]

[1]Department of Environmental and Occupational Health, University of Pittsburgh, Pittsburgh, Pennsylvania 15219

[2]Center for Free Radical and Antioxidant Health, University of Pittsburgh, Pittsburgh, Pennsylvania 15219

[3]Department of Cell Biology, Department of Immunology and Center for Biologic Imaging, University of Pittsburgh, Pittsburgh, Pennsylvania 15219

[4]Department of Critical Care Medicine, and Safar Center for Resuscitation Research, University of Pittsburgh, Pittsburgh, Pennsylvania 15219

[5]Pharmacy College, Jinan University, Guangzhou 510632, China

Introduction

The cell/tissue lipidome comprises over 10,000 individual species of highly diverse molecules.[1, 2] The identification and detailed structural characterization of lipids have been markedly accelerated by the development of soft ionization techniques for mass spectrometry (MS) combined with chromatography.[1, 2] Recently, MS has advanced into the field of imaging to enable the spatial cataloging of lipids in cellular compartments (reviewed in [3, 4]).

The most commonly employed mass spectrometry imaging (MSI) techniques for lipids are secondary ion mass spectrometry (SIMS), desorption electrospray ionization (DESI), and matrix-assisted laser desorption/ionization (MALDI). These techniques have been successfully applied to depict the spatial distribution of endogenous and exogenous molecules, as well as for revealing correlations of the homeostasis of low molecular mass compounds and proteins with disease occurrence.[3–6]

In MALDI-MSI, tissue slices are coated with a matrix that is subsequently ablated by absorbing energy from a laser beam. This desorption forms a plume that also contains intact analyte molecules that were in close proximity to the matrix. The analytes either retain pre-formed charges or engage in charge-transfer reactions in the gas phase.[7, 8] This analysis is repeated at discrete locations on the tissue section, resulting in a “molecular fingerprint” that correlates analyte abundance with spatial location.[3, 4] An intrinsic limitation of MALDI-MSI of lipids is the irregular crystallization of matrices on the analyzed tissue surface.

*To whom correspondence should be addressed.

Variability in the matrix-to-analyte ratio affects ion intensity,[9, 10] an issue that becomes a limiting factor in MALDI-MSI at high lateral resolution.[11] Careful optimization of sample preparation and matrix deposition methods are necessary to achieve the best resolution possible with MALDI imaging.[12–14]

2,5-dihydroxybenzoic acid (DHB) is a widely used matrix for MALDI-MSI of biological molecules, including the mapping of (phospho)lipids.[3, 5] Either sublimation of DHB or dry-coating of DHB crystals through a sieve can give a coating of small crystals over the tissue surface[15, 16]. Spray coating can be optimized to deliver a matrix layer that is fine enough to image individual HeLa cells.[17] As a general rule, smaller matrix crystals and stronger absorbance by the matrix at the laser wavelength yields a more efficient MALDI process, whereby optimal MALDI-MSI is achieved through maximum contact between analytes and matrix molecules.[18]

DHB is a weak acid (pKa = 2.95) that facilitates MALDI-MS detection of lipids that are prone to protonation.[19] For enhanced protonation of analytes, trifluoroacetic acid (TFA; pKa = 0.23) is often used as an additive to DHB. However, recent MALDI-MS studies demonstrated that the combination of DHB/TFA can cause significant hydrolysis of phospholipids.[20]

DHB exhibits a UV spectrum with a maximum at 355 nm, making it a suitable matrix for analyses with MALDI mass spectrometers with N_2 lasers centered at 337 nm. At the optimal analyte-to-matrix ratio, the UV absorbance maximum of DHB should not deviate significantly from the laser wavelength as this would decrease the energy transfer from the laser to the analytes.[18] Optimizing the absorbance of DHB by modifying the aromatic ring with various substituents gives an improved energy transfer.[21] Modifying the physical properties of the matrix will also give improved MALDI-MS performance. Detergents with acid-cleavable alkyl chains have been used to improve the tryptic digestion efficiency of membrane proteins without interfering with MALDI-MS.[13] Matrices with acid-cleavable alkyl chains resulted in a functional detergent-matrix compound that gave greatly improved signals for cell lysates and membrane proteins and generated the unmodified matrix itself upon sample preparation.[14] Noticeably, after cleavage of the alkyl chain, the crystallization properties of the resulting matrix were unchanged from that of the non-alkylated matrix. DHB with various length alkyl chains, when added to another matrix, gave improved signals of up to two orders of magnitude for hydrophobic peptides.[9] The crystallization properties of this mixture of alkylated and non-alkylated matrices were different from that of the non-alkylated matrix alone, and resulted in different distributions of hydrophobic peptides within the sample spot.

In the present study, we have carried out experiments to test whether the introduction of linear hydrocarbon chains in DHB yields matrices with improved analytical characteristics for MALDI-MSI of phospholipids in brain tissue. Targeted synthesis of DHB-C_nH_{2n+1} (C_6H_{13}, C_9H_{19} and $C_{12}H_{25}$) was carried out following the hypothesis that alkyl derivatives of DHB form smaller crystals, which is a pre-requisite for higher spatial resolution, and that incorporation of the alkyl chains of DHB-C_nH_{2n+1} into phospholipid bilayers during matrix deposition on tissue slices will provide better matrix-to-analyte contact.[22, 23]

Materials and Methods

Reagents

All reagents used were purchased from Sigma Chemical Co. (St. Louis, MO). Phospholipid standards including dioleoylphosphatidylserine (DOPS), dioleoylphosphatidyl-ethanolamine (DOPE), dioleoylphosphatidylcholine (DOPC) and 1,1',2,2'-tetraoleoylcardiolipin (TOCL) were purchased from Avanti Polar Lipids (Alabaster, AL, USA).

Alkylation of 2,5-dihydroxybenzoic acid:[24–26]

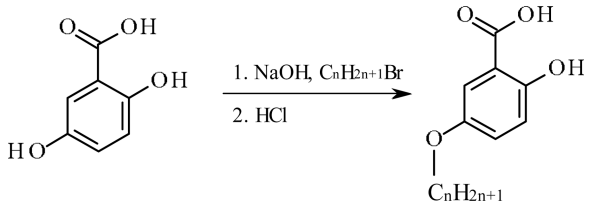

To a vigorously stirred solution of 2,5-dihydrobenzoic acid (3.08 g; 20 mmol) in 12 mL methanol were added dropwise 2 mL of water containing 1.6 g NaOH (40 mmol) and then 4 mL of methanol containing $C_nH_{2n+1}Br$ (23 mmol; n = 6, 9 and 12). After refluxing the reaction solution for 6 hours, the crystals that formed were filtered and re-suspended in dilute HCl at a final pH of 3.0. Crude DHB-C_nH_{2n+1} compounds were extracted with ethyl acetate and the extracts dried over Na_2SO_4. The crystals that formed after rotor-evaporation of the organic solvent were re-crystalized from methanol/water to afford pure DHB-C_nH_{2n+1} (Yield, 75 – 85%). Their purity was verified by LC-MS and they each eluted as one peak at the expected parent masses (*m/z* 237.1, 279.2, and 321.2 for DHB-C_6H_{13}, DHB-C_9H_{19} and DHB-$C_{12}H_{25}$, respectively).

Animal treatment and tissue preparation

All procedures were pre-approved and performed according to the protocols established by the Institutional Animal Care and Use Committee of the University of Pittsburgh. Brains from postnatal day 17 male Sprague Dawley rats were harvested and immediately frozen in liquid nitrogen with neither fixation nor embedding, and were stored at −80°C until sectioning.

Brain tissue was affixed to a cryotome block with minimal Tissue-Tek OCT (Sakura FineTek USA, Torrance CA, USA). The blade and working surfaces of the cryotome were cleaned with methanol immediately prior to cutting, and at no time did the blade come into contact with OCT. Coronal brain sections from Bregma A 2.3 mm to A 3.2 mm were cut at −21 °C to a thickness of 10 μm. These sections were applied to cold histology slides coated with a conductive indium-tin oxide (ITO) surface (Delta Technologies LTD, Loveland, CO, USA). Additional adjacent sections were cut and applied to plain glass slides for conventional histology and total lipid extraction. Lipid extraction from 5.0 mg of dried tissue sections on glass slides was performed using a modified Folch method as described previously.[27] Total lipid extracts were dried under a steady stream of grade 5.0 N_2 then redissolved in 2:1 chloroform:methanol to a total volume of 200 μL and stored at −80°C prior to use.

Matrix application. A Mixture of Four Phospholipids

Solutions of DOPC-DOPE-DOPS-TOCL at a concentration of 0.25 mM each in 2:1 chloroform:methanol were spotted (0.5 μl) onto ITO slides and stored in a glass desiccator using the laboratory vacuum line (100–120 mm Hg) prior to analysis. Solutions of DHB were prepared as 60 mM solutions in 70% methanol and adjusted to the appropriate pH with small amounts of concentrated hydrochloric acid or ammonia. Matrix solutions were applied using a commercial airbrush (Badger Air-Brush Co., Franklin Park, IL, USA) with one second of spray application followed by thirty seconds of drying, repeated for 60 cycles with vacuum drying prior to analysis resulting in a matrix deposition of 100 ± 23 μg/cm^2.

Matrix application. Tissue analyses

DHB-$C_{12}H_{25}$ was prepared as a 30 mM solution in ethanol. Solutions for DHB and DHB-C_6H_{13} were made to 60 mM in 90% methanol and adjusted to the appropriate pH as described above. Solutions of total brain lipid extract were spotted (0.5 μl) onto ITO slides and dried in a glass desiccator using the laboratory vacuum line (100–120 mm Hg) prior to analysis. As in the method reported by Chen et al.,[28] matrix deposition onto tissue sections and total lipid extracts were performed with a capillary spraying device constructed in house (see below). The amount of matrix deposition was adjusted by varying the deposition times while maintaining a constant flow of matrix solution. Tissue sections were dried at 4°C under vacuum (2 mm Hg) both prior to and immediately after matrix deposition, and stored at 4°C in a glass desiccator under vacuum prior to analysis.

Instrumentation

MALDI time-of-flight (TOF) -MS and –MSI analyses were performed using a Bruker Ultraflex II TOF/TOF mass spectrometer equipped with a MNL-100 337 nm wavelength N_2 laser (Bruker Daltonics, Billerica, MA, USA). Spectral acquisition and analysis was performed using FlexControl 3.3 and FlexAnalysis 3.3 software (Bruker Daltonics, Billerica, MA, USA). Laser energy was measured at 112μJ (standard deviation of 1.4μJ) and attenuation adjustment was set by the software with an allowable range between 60% and 80% of full transmission. Therefore 100% laser energy (minimum attenuation) corresponds to 89.6μJ and 0% laser energy (maximum attenuation) corresponds to 67.2μJ. In order to apply matrix more homogenously than airbrushes or TLC sprayers can achieve, we have constructed a capillary-sprayer from the electrospray source from a Thermo-Finnigan TSQ 7000 mass spectrometer. The existing capillary was replaced with a 75 micron i.d. polyimide coated capillary tubing. Sheath gas (grade 5.0 N_2) was regulated to 80 psi at the output of the nitrogen regulator. Further fine control of nitrogen gas was achieved with a needle valve to achieve a flow of 30 L/h. The spray nozzle was positioned 23 mm above the tissue. A syringe pump delivered matrix solution at a rate of 2.0 μL/min. This combination of gas flow, height and deposition rate has been used to attain coating of the tissue sections with approximately 45 μg of matrix per cm^2, which is similar to the optimal deposition range of 50–180 μg/cm^2 observed with sublimation.[29]

Tissue analysis

MALDI-MS and –MSI spectra were acquired in reflector mode with either positive or negative polarity depending on the experiment. A matrix deflection cut-off of up to 400 Da was used. MALDI-MSI images were acquired at a raster step size of 50 μm, with a summation of 30 laser shots per location at a pulse repetition rate of 20 Hz. Depending on the image size, acquisition took between 30 min to 2 hours. In order to maximize signal intensity, random walking was performed every two laser shots within each location. These settings gave the best compromise among signal intensity, matrix depletion, and acquisition time. Spatial locations for MALDI-MSI were determined by co-registering fiducial markers on optical images acquired from a microscope prior to matrix deposition. Histological locations on the brain tissue were determined by consulting *The Rat Brain in Stereotaxic Coordinates*.[30] MALDI-MSI images were produced from the corresponding spectra to generate a relative intensity ion map at a given *m/z* value using FlexImaging 3.0 (Bruker Daltonics, Billerica, MA, USA) without normalization.

Results

To assess the effects of H^+ on MALDI-MS of phospholipids, we have performed analyses with DHB solutions of varying acidity (pH = 2 – 8). In this pH range phospholipids do not undergo hydrolysis to any significant extent. However at pH > 4 the carboxylic group of DHB is fully deprotonated and, at 335 nm, its anionic form absorbs approximately 30% less light than the protonated acid (Supplementary Information (SI); figure 1S). Because the buffer potential of most tissues is centered at semi-neutral pH values, the deposition of DHB (after evaporation of the solvent) on tissue slices for MALDI-MSI of lipids may lead to deprotonation of the matrix thereby decreasing analytical sensitivity.

Figure 1 shows the MALDI-MS profiles of an equimolar mixture of 1,2-dioleoylphosphatidylcholine (DOPC; $[M + H]^+$, *m/z* = 786.5; $[M + Na]^+$, *m/z* = 808.4), 1,2-dioleoylphosphatidylethanolamine (DOPE; $[M + H]^+$, *m/z* = 744.5; $[M + Na]^+$, *m/z* = 766.4), 1,1',2,2'-tetraoleoyl cardiolipin (TOCL; $[M - H]^-$, *m/z* = 1456.1; $[M - 2H + Na]^-$, *m/z* = 1479.1) and 1,2-dioleoylphosphatidylserine (DOPS; $[M – H]^-$, *m/z* = 786.6) obtained at 25% laser energy (LE). In both the positive (Fig. 1A) and negative (Fig. 1B) modes of ionization, maximum peak intensities were attained from samples prepared with solutions of DHB at pH 2 (Fig. 2A,D). By varying the LE, peak intensities followed biphasic distributions with maxima at 30% and 45% LE for samples coated with DHB at pH 2 and 4.7, respectively (Fig. 2B,C,E,F). In positive ionization mode at optimal LE, peak intensities decreased up to 50% at pH 4.7 (as compared to pH 2). In the negative mode, no significant changes in sensitivity were observed by varying the pH (Fig. 1, B and E compared to C and F, respectively).

We next conducted comparative MALDI-MS analyses of phospholipids in thin (10 micron) tissue slices from rat brain coated with DHB, DHB-C_6H_{13} and DHB-$C_{12}H_{25}$. For each matrix, analytical sensitivity in the negative ion mode was optimized by tuning the laser energy to give the maximum peak intensity of the ion at *m/z* 806.5 (Fig. 3). Notably, at optimal analytical sensitivity for DHB (45% LE), no desorption/ionization of phospholipids by either DHB-C_6H_{13} or DHB-$C_{12}H_{25}$ was detected from tissue. These data may be of

relevance to studies by Fukuyama et al., who recently reported that DHB-C_8H_{17} does not produce MALDI mass spectra of hydrophobic peptides; but the addition of DHB-C_8H_{17} to a conventional matrix, α-cyano-4-hydroxycinnamic acid, increased the sensitivity of MALDI analysis by 2 orders of magnitude.[9] In our model, comparable analytical sensitivity for lipids in negative ion mode was attained with DHB, DHB-C_6H_{13} and DHB-$C_{12}H_{25}$ at LE of 45%, 60%, and 60%, respectively (Figure 4). LE higher than 65% were not used because of baseline shifts and fragmentation of analytes (data not shown). There was little difference in the spectral quality of lipid profiles obtained directly from tissues slices (Fig. 4A) and purified extracts from these tissues (Fig. 4B). Therefore, endogenous salts and proteins, which are present in tissue slices but not in purified extracts, did not strongly interfere with the analysis. Based on published data, assignments of the observed species are presented in Table 1. The most prominent species detected were sulfatides (ST(d18:1/18:0), ST(d18:1/24:1), and ST(d18:1/24:0) at *m/z* 806.6, 888.6, and 890.6 respectively) hydroxyl-sulfatides (ST(d18:1/h24:1) and ST(d18:1/h24:0) at *m/z* 904.6 and 906.6, respectively), and phosphatidylinositol (PI(38:4), *m/z* 885.5).

To test the hypothesis that alkylated hydrophobic derivatives of DHB may produce smaller crystals, DHB, DHB-C_6H_{13}, and DHB-$C_{12}H_{25}$ were deposited on brain slices and the structure of the coatings were examined (Fig. 5, panels A, B and C, respectively) using differential interference contrast microscopy (DIC, sub-panels i-iii of each) and polarized light microscopy (sub-panels iv-vi). The total zoomed image in panel ii corresponds to the area shown in the red box in panel i, and the same with the red box in panel ii giving panel iii. A trend of transition from crystals to oily surfaces is apparent in the sequence DHB → DHB-C_6H_{13} → DHB-$C_{12}H_{25}$, with DHB-C_6H_{13} forming fewer (and smaller) visible crystals than DHB (panel A compared to panel B).

Figure 6 presents typical MALDI-MSI ion maps of lipids from brain tissue sections coated with DHB and DHB-$C_{12}H_{25}$. An optical image of a near-serial tissue section (Figure 6A) shows the locations on opposite hemispheres that were coated with DHB and DHB-$C_{12}H_{25}$ and subsequently analyzed with MALDI-MSI (black rectangles). Individual MALDI-MS spectra were recorded with a lateral (X-Y) resolution[1] of 50 μm (Figure 6B) in negative ionization mode and at optimal LE. The MALDI ion images with *m/z* values of 806, 822, 862, 888, 904 and 906 obtained with DHB contained large areas were none of these analytes were detected or were below the sensitivity threshold. In contrast, DHB-$C_{12}H_{25}$ depicted a more continuous distribution of these analytes. These data indicate that DHB-$C_{12}H_{25}$ affords higher lateral resolution than DHB.

Discussion

The main finding of this study is that in MALDI-MSI of lipids, DHB-$C_{12}H_{25}$ is a matrix that affords higher analytical sensitivity/lateral resolution than DHB. Ion maps of select analytes using DHB-$C_{12}H_{25}$ displayed a relatively continuous distribution. On the other hand, the MALDI ion images of these analytes obtained with DHB contained large areas that were devoid of signal.

[1]Spatial (lateral) resolution is the distance between adjacent pixels or ablated spots on the sample surface.

MALDI-MSI is a highly-sensitive imaging technique that allows the analysis of the spatial distribution of biomolecules.[4] Among numerous biomolecular targets, lipids have been the focus of much MALDI-MSI research because of their relative abundance (at least for most lipids) in tissue making them excellent candidates for imaging. In addition, the molecular diversity of lipids allows them to perform essential structural, modulating and signaling functions in cells and tissues making them highly desirable imaging targets.[31, 32] Recent MALDI-MSI studies of lipids led to the development of protocols that afforded higher spatial resolution and addressed the possibility for introduction of quantitative criteria for data analysis.[10, 33, 34]

Obtaining better spatial resolution is critical for the analysis of sub-anatomical structures and site-specific metabolic reactions. In general, particle beam methods provide better resolved MS images as compared to MALDI-MSI. Although MALDI-MSI resolution is limited by the laser spot diameter, an oversampling method that allows analysis of areas smaller than the laser spot has been developed by Jurchen et al.[33] The method is based on the screening of the analyzed surface, with complete ablation of the MALDI matrix at each sample position, following a lateral shift of the laser spot to the next location at a distance less than the diameter of the laser beam.[33]

In addition to optical limitations, the inherent variability of MALDI signals from lipids within tissue slices is related to the heterogeneity of both the sample surface and the matrix crystallization.[35] Often matrices crystalize in clusters and illumination of matrix-free areas results in the loss of signal. To circumvent some of these limitations, at least in part, we synthesized improved matrices for lipid analysis based on structural modifications of DHB that do not affect its UV absorbance but change its physical properties.

In a typical spray-deposition MALDI-MSI experiment, tissue sections are sprayed with a solution containing matrix. In turn, evaporation of the solvent leads to crystallization of the matrix on the analyzed surface. Dry-coating of tissue for MALDI-MSI can be achieved by sublimation or sieve-deposition to deliver crystals of matrix to the tissue without solvent. Various other matrix deposition methods include robotic and inkjet spotting, electrospray deposition, and airbrush or capillary spray (ref. [36] and the references therein). Comparative microphotographs of tissue sections coated with DHB by these methods show that DHB can crystalize in clusters that are separated by uncoated tissue areas with lengths of up to 100 μm.[36–38] Optimal MALDI-MS spectra are obtained from areas with a high density of matrix crystals,[9, 39] whereby the mass spectral peak intensity, resolution and reproducibility are inversely proportional to the heterogeneity of the matrix coating. The imaging of biological systems that are smaller than the DHB clusters can be achieved with high resolution. For example, Schober et al. detected lipids from a single cell (length, ~ 100 μm) with a resolution of ~ 7 μm.[17] However, when imaging tissue sections with a length of several centimeters is carried out, the clustering of DHB can affect the intensity of the MS spectra [6, 26]. Recently, Hankin et al. have reported that the application of DHB on brain tissue slices by sublimation of the matrix affords a coating with small crystals that do not form clusters.[15] The latter method is based on the heating of DHB to 120 °C at reduced pressure (0.05 Torr) with concomitant condensation/crystallization of DHB vapors on the analyzed tissue sections. Optimization of the amount of matrix that condenses on the

analyzed surface requires careful adjustment of experimental parameters such as pressure, the amount of heat applied to the matrix and the time of sublimation,[29] with appropriate controls to determine that the analyzed surface has not been perturbed by overheating. The coating of tissue samples with DHB by the sublimation method has allowed MALDI-MSI of lipids with a spatial resolution of approximately 10 μm.[11]

We have targeted the synthesis of DHB-C_nH_{2n+1} (C_6H_{13}, C_9H_{19} and $C_{12}H_{25}$) following the rationale that alkyl derivatives of DHB would form smaller crystals than DHB, which is a pre-requisite for higher lateral resolution analyses, and that incorporation of the alkyl chains of DHB-C_nH_{2n+1} into phospholipid bilayers (detergent effect) during spray deposition on tissue slices will provide better matrix-to-analyte contact. We hypothesized that DHB-C_nH_{2n+1} would form smaller crystals following the empirical observation that the melting points of *O*-alkylated phenolic compounds decrease with increases in the length of their alkyl chains. For example, the melting points of 2-hydroxybenzoic (salicylic) acid, 2-methoxybenzoic acid and 2-ethoxybenzoic acid are 158 °C, 101 °C and 19 °C, respectively. The observed decreases in the melting points can be correlated with the decrease in polarity of the corresponding derivatives. Further, assuming that the crystal growth in this example obeys Gibbs' rules of phase equilibria at constant pressure, it is reasonable to speculate that the transition from crystalline to liquid phase will reflect shifts in these equilibria that include the formation of smaller crystals (as opposed to crystal growth). It is noteworthy that *O*-alkylation of DHB to DHB-C_nH_{2n+1} does not significantly affect the UV spectrum of this matrix. In ethanol, DHB, DHB-C_6H_{13} and DHB-$C_{12}H_{25}$ exhibit UV spectra with maximal absorptions at 333 nm, 229 nm, and 229 nm, respectively; for all matrices, $\varepsilon \simeq 3.2 \times 10^3$ $M^{-1}.cm^{-1}$).

On rat brain tissue sections, our spray deposition system produced DHB crystals of approximately 20 μm in length that were grouped in clusters spaced by areas of uncoated tissue sections (Fig. 5Aiv). DHB-C_nH_{2n+1} exhibited a trend of transition from crystals to an oily layer in the sequence DHB → DHB-C_6H_{13} → DHB-$C_{12}H_{25}$, with DHB-C_6H_{13} forming less (and smaller) crystals than DHB (panel A compared to panel B). Comparison of the data presented in Fig. 6A and 5C.i., and Fig. 2S and 3S (SI), indicates that DHB-$C_{12}H_{25}$ did not cause any apparent structural changes in the analyzed tissue sections. Both DHB-C_6H_{13} and DHB-$C_{12}H_{25}$ required a higher LE than DHB for the detection of peaks with comparable intensities, which correlates with the increased boiling points (b.p.) of the *O*-alkylated matrices; at 25 °C and 760 mm Hg, the b.p. of DHB, DHB-C_6H_{13} and DHB-$C_{12}H_{25}$ are 367.33 °C, 414.03 °C and 490.29 °C (estimations made with ChemDraw Ultra, v. 12). Although the algorithm used for b.p. estimations provides only approximate values,[40] it denotes the expected trend of increased temperatures for the phase transition of the alkylated matrices. In MALDI experiments, analytes are in contact with matrix molecules, which are then irradiated with high energy laser pulses. This triggers the evaporation of matrix and analyte molecules as ionized molecular species. Vertes et al. proposed that this process proceeds via an initial bulk-desorption of the matrix with concomitant energy transfer to analytes.[41] It has been further discussed that the mechanical process of desorption activates analyte molecules via transfer of a reaction momentum in the gas phase (“Popcorn” model).[42] Alternatively, competitive kinetics between sublimation and fragmentation have

been considered ("Bottle-neck" model), whereby a "good" matrix has been postulated to possess a low phase-transition temperature.[41, 43] Studies by Price et al., however, have shown that the enthalpy of matrix evaporation/sublimation is not the principle factor in the MALDI process.[44] In our analysis of lipids with DHB and its *O*-alkyl derivatives, we were able to compensate for differences in MALDI sensitivity by increasing the LE. Importantly, DHB-$C_{12}H_{25}$ was layered exclusively as oil on the tissues sections, which suggests that it provided a more complete, homogenous coating of the analyzed surface. Indeed, comparative MSI analysis of lipids in brain tissues with DHB and DHB-$C_{12}H_{25}$ indicated that the latter matrix affords better lateral resolution (Fig. 6).

Our results indicate that *O*-alkylation of DHB for MALDI-MSI is a promising approach for enhanced spatial resolution. Since hydroxy and amino functions on aromatic ring systems are common functional groups that are the key to the usefulness of several widely used matrices, such as 9-aminoacridine, α-cyano-4-hydroxycinnamic acid, sinapic acid, 2,6-dihydroxyacetophenone, and 1,5-diaminonaphtalene, perhaps O- and N-alkylation may be suitable approaches for modifying these matrices. Currently, the factors that affect the crystallization of these matrices on tissue sections are not well understood and require further study.

Supplementary Material

Refer to Web version on PubMed Central for supplementary material.

Acknowledgments

This study was supported in part by grants from the US National Institutes of Health (NS076511 and U19AI068021 (H.B., V.E.K. and D.A.S.), ES021068 (B.R.P. and V.E.K.), NS061817 (H.B.), ES020693 (V.E.K.), U54 GM103529 08 (S.C.W.)), the US National Institute for Occupational Safety and Health (OH008282 to V.E.K.). This project used the UPCI Cancer Biomarkers Facility that is supported in part by Cancer Center Support Grant (CCSG) P30CA047904.

References

1. Dennis EA. Lipidomics joins the omics evolution. Proc Natl Acad Sci U S A. 2009; 106:2089. [PubMed: 19211786]
2. Griffiths WJ, Wang Y. Mass spectrometry: from proteomics to metabolomics and lipidomics. Chem Soc Rev. 2009; 38:1882. [PubMed: 19551169]
3. Norris JL, Caprioli RM. Analysis of tissue specimens by matrix-assisted laser desorption/ionization imaging mass spectrometry in biological and clinical research. Chem Rev. 2013; 113:2309. [PubMed: 23394164]
4. Gode D, Volmer DA. Lipid imaging by mass spectrometry - a review. Analyst. 2013; 138:1289. [PubMed: 23314100]
5. Berry KA, Hankin JA, Barkley RM, Spraggins JM, Caprioli RM, Murphy RC. MALDI imaging of lipid biochemistry in tissues by mass spectrometry. Chem Rev. 2011; 111:6491. [PubMed: 21942646]
6. Fuchs B, Suss R, Schiller J. An update of MALDI-TOF mass spectrometry in lipid research. Prog Lipid Res. 2010; 49:450. [PubMed: 20643161]
7. Jaskolla TW, Karas M. Compelling evidence for Lucky Survivor and gas phase protonation: the unified MALDI analyte protonation mechanism. J Am Soc Mass Spectrom. 2011; 22:976. [PubMed: 21953039]
8. Dreisewerd K. The desorption process in MALDI. Chem Rev. 2003; 103:395. [PubMed: 12580636]

9. Fukuyama Y, Tanimura R, Maeda K, Watanabe M, Kawabata S, Iwamoto S, Izumi S, Tanaka K. Alkylated dihydroxybenzoic acid as a MALDI matrix additive for hydrophobic peptide analysis. Anal Chem. 2012; 84:4237. [PubMed: 22506777]
10. Landgraf RR, Garrett TJ, Conaway MC, Calcutt NA, Stacpoole PW, Yost RA. Considerations for quantification of lipids in nerve tissue using matrix-assisted laser desorption/ionization mass spectrometric imaging. Rapid Commun Mass Spectrom. 2011; 25:3178. [PubMed: 21953974]
11. Chaurand P, Cornett DS, Angel PM, Caprioli RM. From whole-body sections down to cellular level, multiscale imaging of phospholipids by MALDI mass spectrometry. Mol Cell Proteomics. 2011; 10 O110 004259.
12. Teuber K, Schiller J, Fuchs B, Karas M, Jaskolla TW. Significant sensitivity improvements by matrix optimization: a MALDI-TOF mass spectrometric study of lipids from hen egg yolk. Chem Phys Lipids. 2010; 163:552. [PubMed: 20420816]
13. Yu YQ, Gilar M, Gebler JC. A complete peptide mapping of membrane proteins: a novel surfactant aiding the enzymatic digestion of bacteriorhodopsin. Rapid Commun Mass Spectrom. 2004; 18:711. [PubMed: 15052583]
14. Norris JL, Porter NA, Caprioli RM. Combination detergent/MALDI matrix: functional cleavable detergents for mass spectrometry. Anal Chem. 2005; 77:5036. [PubMed: 16053319]
15. Hankin JA, Barkley RM, Murphy RC. Sublimation as a method of matrix application for mass spectrometric imaging. J Am Soc Mass Spectrom. 2007; 18:1646. [PubMed: 17659880]
16. Puolitaival SM, Burnum KE, Cornett DS, Caprioli RM. Solvent-free matrix dry-coating for MALDI imaging of phospholipids. J Am Soc Mass Spectrom. 2008; 19:882. [PubMed: 18378160]
17. Schober Y, Guenther S, Spengler B, Rompp A. Single cell matrix-assisted laser desorption/ ionization mass spectrometry imaging. Anal Chem. 2012; 84:6293. [PubMed: 22816738]
18. Trimpina S, Räderb HJ, Müllen K. Investigations of theoretical principles for MALDI-MS derived from solvent-free sample preparation: Part I. Preorganization. International Journal of Mass Spectrometry. 2006; 253:13.
19. Schiller J, Suss R, Fuchs B, Muller M, Petkovic M, Zschornig O, Waschipky H. The suitability of different DHB isomers as matrices for the MALDI-TOF MS analysis of phospholipids: which isomer for what purpose? Eur Biophys J. 2007; 36:517. [PubMed: 17047951]
20. Schiller J, Muller K, Suss R, Arnhold J, Gey C, Herrmann A, Lessig J, Arnold K, Muller P. Analysis of the lipid composition of bull spermatozoa by MALDI-TOF mass spectrometry--a cautionary note. Chem Phys Lipids. 2003; 126:85. [PubMed: 14580713]
21. Wiegelmann M, Soltwisch J, Jaskolla TW, Dreisewerd K. Matching the laser wavelength to the absorption properties of matrices increases the ion yield in UV-MALDI mass spectrometry. Anal Bioanal Chem. 2013; 405:6925. [PubMed: 23064675]
22. Kagan VE, Serbinova EA, Koynova GM, Kitanova SA, Tyurin VA, Stoytchev TS, Quinn PJ, Packer L. Antioxidant action of ubiquinol homologues with different isoprenoid chain length in biomembranes. Free Radic Biol Med. 1990; 9:117. [PubMed: 2227528]
23. Kamaya H, Kaneshina S, Ueda I. Partition equilibrium of inhalation anesthetics and alcohols between water and membranes of phospholipids with varying acyl chain-lengths. Biochim Biophys Acta. 1981; 646:135. [PubMed: 7272298]
24. Baganz H, Krattner R. New gentisic acid derivatives. Archiv der Pharmazie und Berichte der Deutschen Pharmazeutischen Gesellschaft. 1960; 293:393.
25. Fan X, Zhang FH, Al-Safi RI, Zeng LF, Shabaik Y, Debnath B, Sanchez TW, Odde S, Neamati N, Long YQ. Design of HIV-1 integrase inhibitors targeting the catalytic domain as well as its interaction with LEDGF/p75: a scaffold hopping approach using salicylate and catechol groups. Bioorg Med Chem. 2011; 19:4935. [PubMed: 21778063]
26. Evans JC, Klix RC, Bach RD. Diels-Alder Approaches to Model Compounds Related to Fredericamycin A. J. Org. Chem. 1988; 53:5519.
27. Tyurina YY, Kisin ER, Murray A, Tyurin VA, Kapralova VI, Sparvero LJ, Amoscato AA, Samhan-Arias AK, Swedin L, Lahesmaa R, Fadeel B, Shvedova AA, Kagan VE. Global phospholipidomics analysis reveals selective pulmonary peroxidation profiles upon inhalation of single-walled carbon nanotubes. ACS Nano. 2011; 5:7342. [PubMed: 21800898]

28. Chen Y, Liu Y, Allegood J, Wang E, Cachon-Gonzalez B, Cox TM, Merrill AH Jr, Sullards MC. Imaging MALDI mass spectrometry of sphingolipids using an oscillating capillary nebulizer matrix application system. Methods Mol Biol. 2010; 656:131. [PubMed: 20680588]
29. Thomas A, Charbonneau JL, Fournaise E, Chaurand P. Sublimation of new matrix candidates for high spatial resolution imaging mass spectrometry of lipids: enhanced information in both positive and negative polarities after 1,5-diaminonapthalene deposition. Anal Chem. 2012; 84:2048. [PubMed: 22243482]
30. Paxinos, G.; Watson, C. The Rat Brain in Stereotaxic Coordinates. San Diego, California, USA: Academic Press, Inc.; 1997.
31. Brown HA, Murphy RC. Working towards an exegesis for lipids in biology. Nat Chem Biol. 2009; 5:602. [PubMed: 19690530]
32. Shevchenko A, Simons K. Lipidomics: coming to grips with lipid diversity. Nat Rev Mol Cell Biol. 2010; 11:593. [PubMed: 20606693]
33. Jurchen JC, Rubakhin SS, Sweedler JV. MALDI-MS imaging of features smaller than the size of the laser beam. J Am Soc Mass Spectrom. 2005; 16:1654. [PubMed: 16095912]
34. Angel PM, Spraggins JM, Baldwin HS, Caprioli R. Enhanced sensitivity for high spatial resolution lipid analysis by negative ion mode matrix assisted laser desorption ionization imaging mass spectrometry. Anal Chem. 2012; 84:1557. [PubMed: 22243218]
35. Schiller J, Suss R, Fuchs B, Muller M, Zschornig O, Arnold K. MALDI-TOF MS in lipidomics. Front Biosci. 2007; 12:2568. [PubMed: 17127263]
36. Baluya DL, Garrett TJ, Yost RA. Automated MALDI matrix deposition method with inkjet printing for imaging mass spectrometry. Anal Chem. 2007; 79:6862. [PubMed: 17658766]
37. Aerni HR, Cornett DS, Caprioli RM. Automated acoustic matrix deposition for MALDI sample preparation. Anal Chem. 2006; 78:827. [PubMed: 16448057]
38. Trimpin S, Herath TN, Inutan ED, Wager-Miller J, Kowalski P, Claude E, Walker JM, Mackie K. Automated solvent-free matrix deposition for tissue imaging by mass spectrometry. Anal Chem. 2010; 82:359. [PubMed: 19968249]
39. Pan C, Xu S, Zhou H, Fu Y, Ye M, Zou H. Recent developments in methods and technology for analysis of biological samples by MALDI-TOF-MS. Anal Bioanal Chem. 2007; 387:193. [PubMed: 17086385]
40. Mills N. Computer software reviews. J. Am. Chem. Soc. 2005; 128:13649.
41. Vertes A, Gijbels R, Levine R. Homogeneous Bottleneck Model of Matrix-assisted Ultraviolet Laser Desorption of Large Molecules. Rapid Comm. Mass. Spec. 1990; 4:228.
42. Williams P, Sundqvist B. Mechanism of Sputtering of Large Biomolecules by Impact of Highly Ionizing Particles. Phys. Rev. Lett. 1986; 58:1031. [PubMed: 10034314]
43. Vertes A, Levine RD. Sublimation versus fragmentation in matrix-assisted laser desorption. Chem. Phys. Lett. 1990; 171:284.
44. Price PM, Bashir S, Derrick PR. Sublimation properties of x,y-dihydroxybenzoic acid isomers as model matrix assisted laser desorption ionisation (MALDI) matrices. Thermochimica Acta. 1999; 327:167.
45. Hsu FF, Bohrer A, Turk J. Electrospray ionization tandem mass spectrometric analysis of sulfatide. Determination of fragmentation patterns and characterization of molecular species expressed in brain and in pancreatic islets. Biochim Biophys Acta. 1998; 1392:202. [PubMed: 9630631]

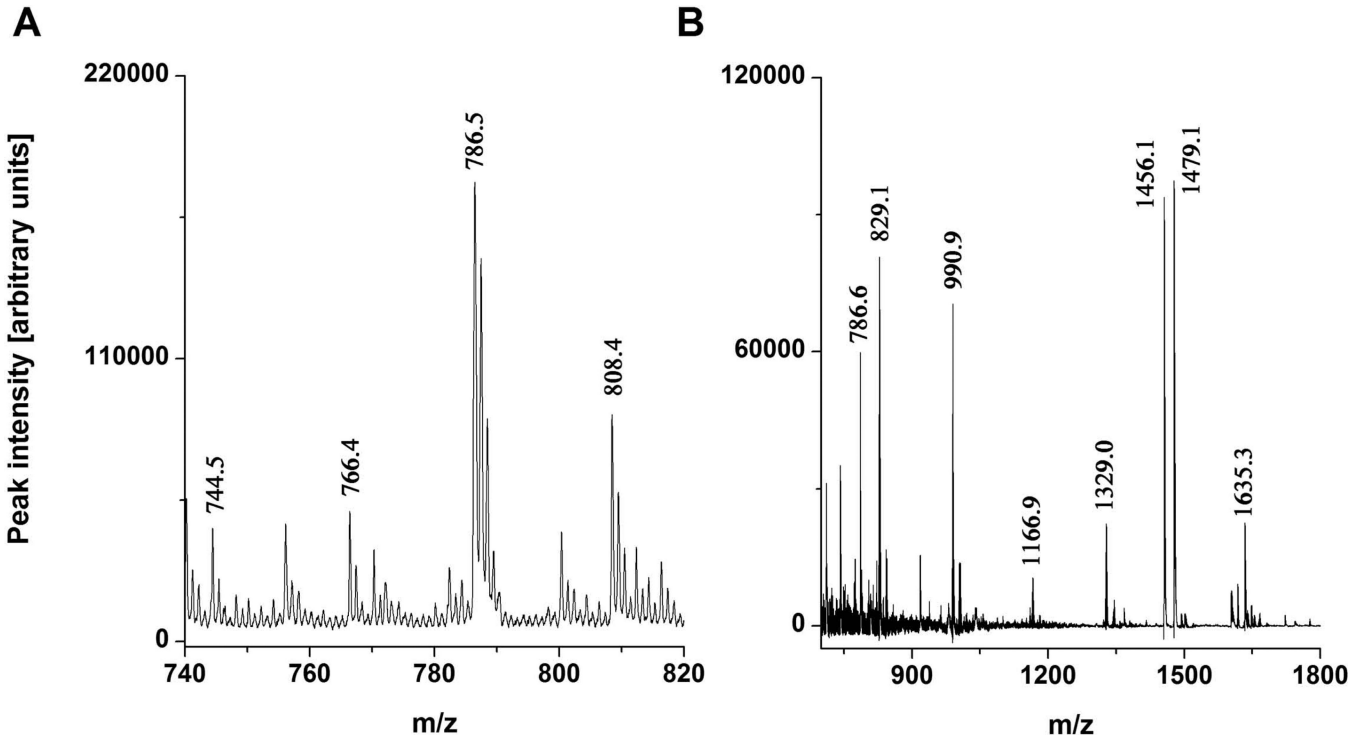

Figure 1. Representative MALDI-MS spectra of a standard lipid mixture

A standard lipid mixture was spotted and overlaid with solution of DHB adjusted to pH 2.0. In positive ion mode (**panel A**), DOPE is detected as both $[M+H]^+$ and $[M+Na]^+$ at *m/z* 744.5 and 766.4, respectively. DOPC is detected as both $[M+H]^+$ and $[M+Na]^+$ at *m/z* 786.5 and 808.4, respectively. In negative ion mode (**panel B**) DOPS is detected as $[M-H]^-$ at *m/z* 786.6, and TOCL is detected as both $[M-H]^-$ and $[M-2H+Na]^-$ at *m/z* 1456.1 and 1479.1, respectively.

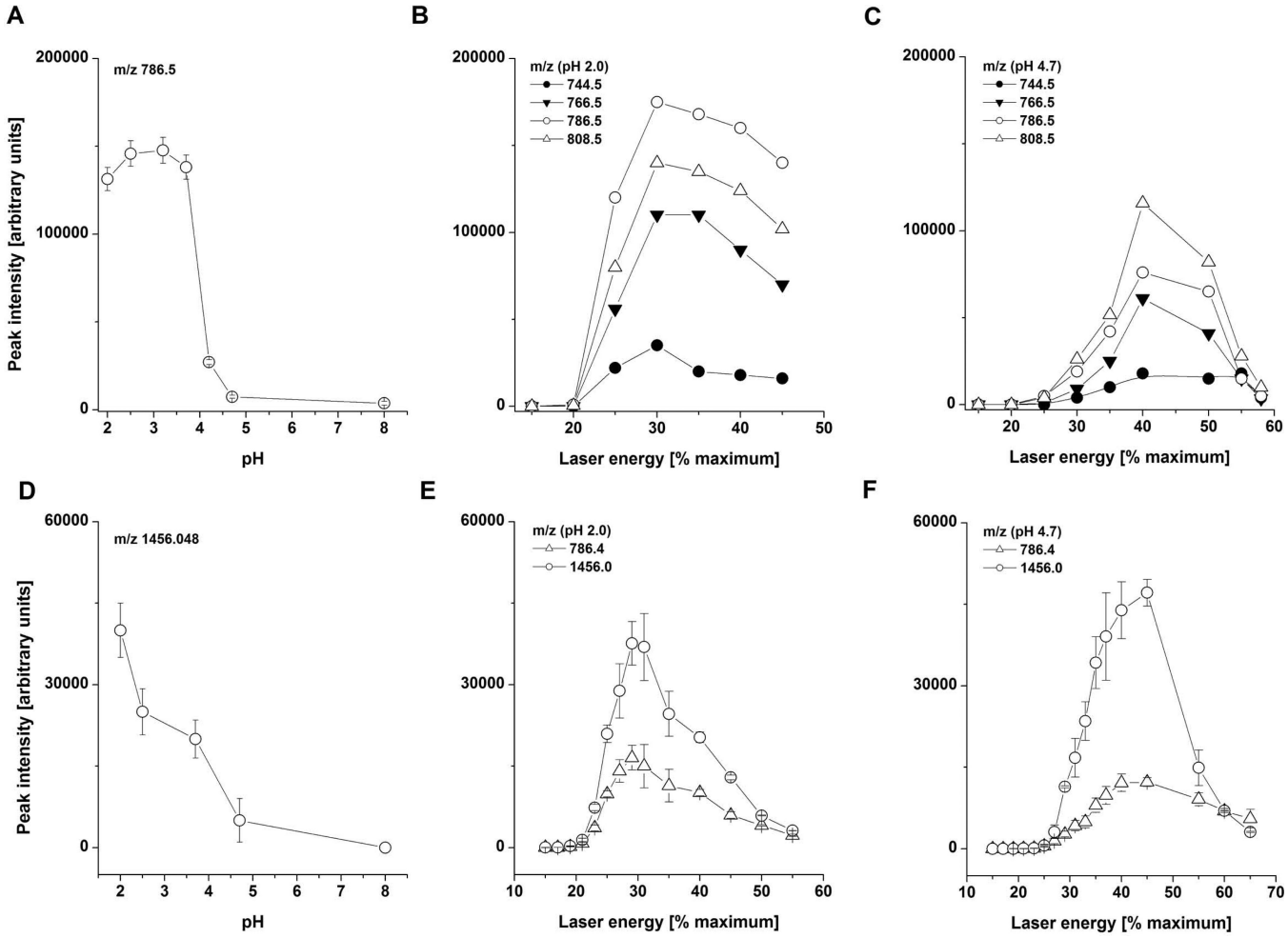

Figure 2.

Effects of pH and LE on ion intensity. Peak intensities for lipid standards were assessed in both positive (panels A-C) and negative (panels D-F) ion modes. The peak intensities for DOPC (*m/z* 786.5 as $[M+H]^+$, panel A) were assessed at various pH values at constant LE of 24%. The peak intensities for DOPE (both $[M+H]^+$ and $[M+Na]^+$ at *m/z* 744.5 and 766.4, respectively) and DOPC (both $[M+H]^+$ and $[M+Na]^+$ at *m/z* 786.5 and 808.4, respectively) were assessed by holding the pH constant at either 2.0 (panel B) or 4.7 (panel C) while varying the LE. The peak intensities for TOCL (*m/z* 1456.1 as $[M-H]^-$, panel D) were then assessed at various pH values at a constant LE of 24%. The peak intensities for DOPS (*m/z* 786.4 as $[M-H]^-$) and TOCL (*m/z* 1456.1 as $[M-H]^-$) were assessed by holding the pH constant at either 2.0 (panel E) or 4.7 (panel F) while varying the LE.

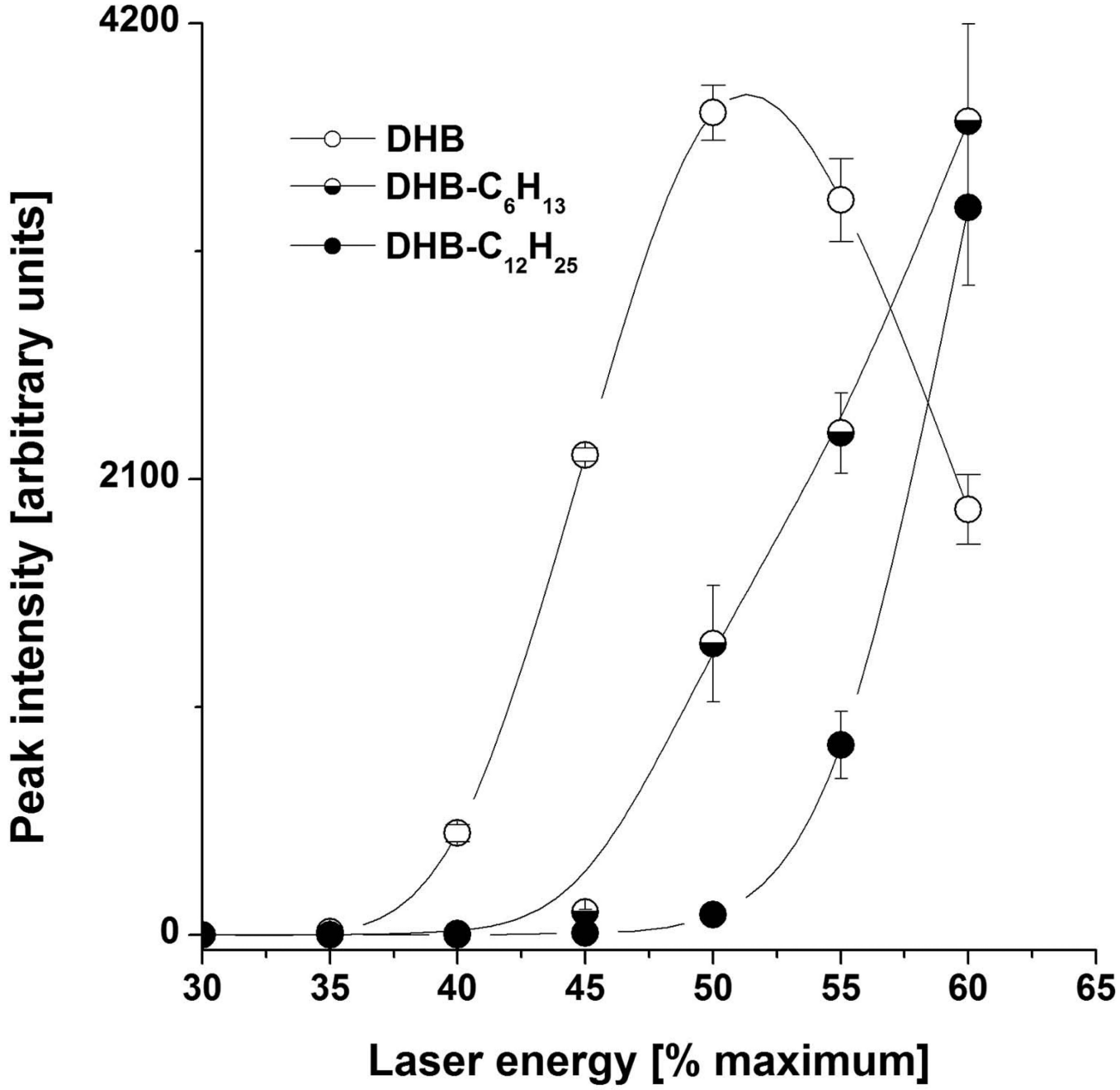

Figure 3. Peak intensity as a function of LE for different matrices

Three tissue sections were prepared with DHB, DHB-C_6H_{13}, and DHB-$C_{12}H_{25}$ and similar locations on the white matter region in each were analyzed at increasing LE. The intensity of the ion at *m/z* 806.5 (ST(d18:1/18:0)) was compared among all three matrices.

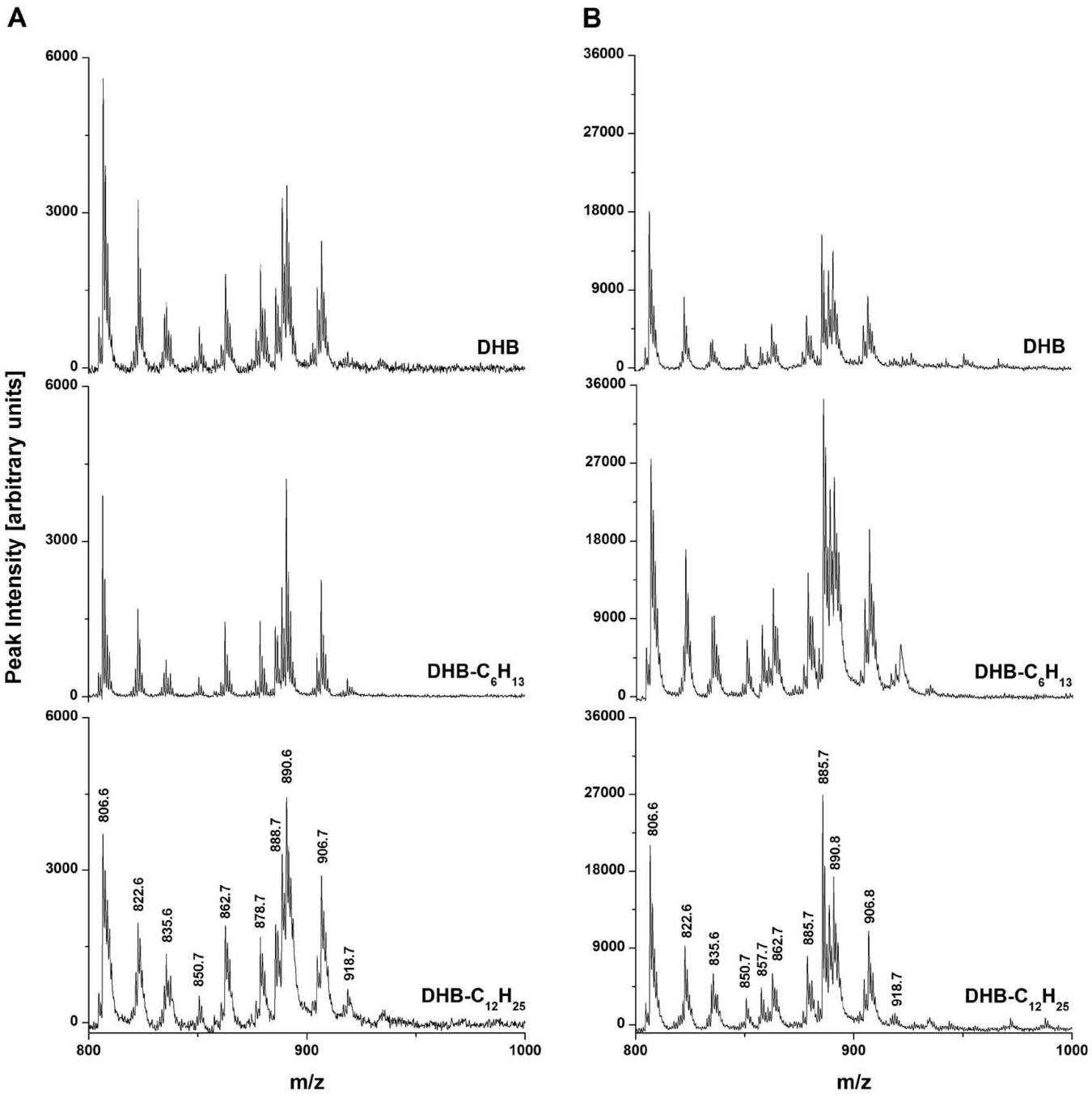

Figure 4. MALDI-MS lipid spectra of capillary-sprayed matrix on tissue slices and lipid extracts from rat brain

Both brain tissue (column A) and brain lipid extracts (column B) were coated with DHB-C_nH_{2n+1} solutions using a capillary-sprayer and analyzed at optimal LE in negative ion mode. Spectra for tissue slices were acquired from MALDI-MSI of a 200 micron location on the white matter region as summation of 30 laser shots, while MALDI-MS of lipid extracts were a summation of 200 laser shots.

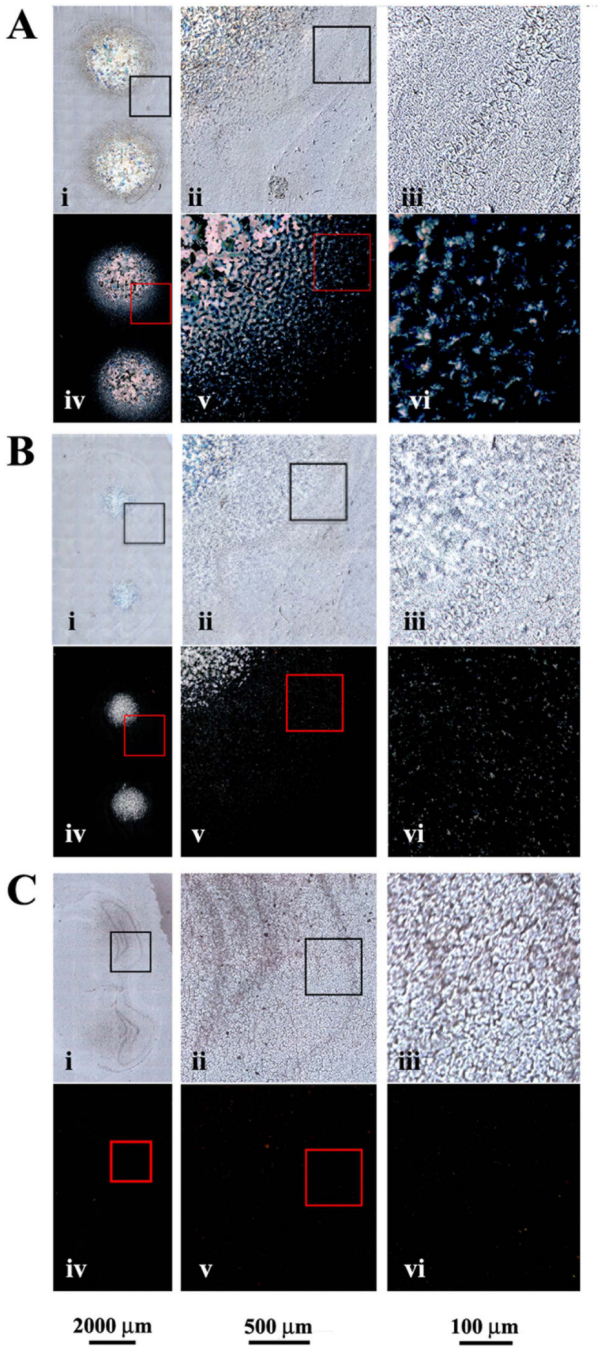

Figure 5. Physical coating properties of different matrices deposited on tissue

DHB (panel A), DHB-C_6H_{13} (panel B) and DHB-$C_{12}H_{25}$ (panel C) were deposited on two locations on tissue and examined with polarized light microscopy (sub-panels i-iii of each) and differential interference contrast microscopy (DIC, sub-panels iv-vi). The red box in panel i of each matrix is the total zoomed image in panel ii, and the same with the red box in panel ii giving panel iii. Likewise the red boxes in panels iv and v give the entire images of panels v and vi, respectively.

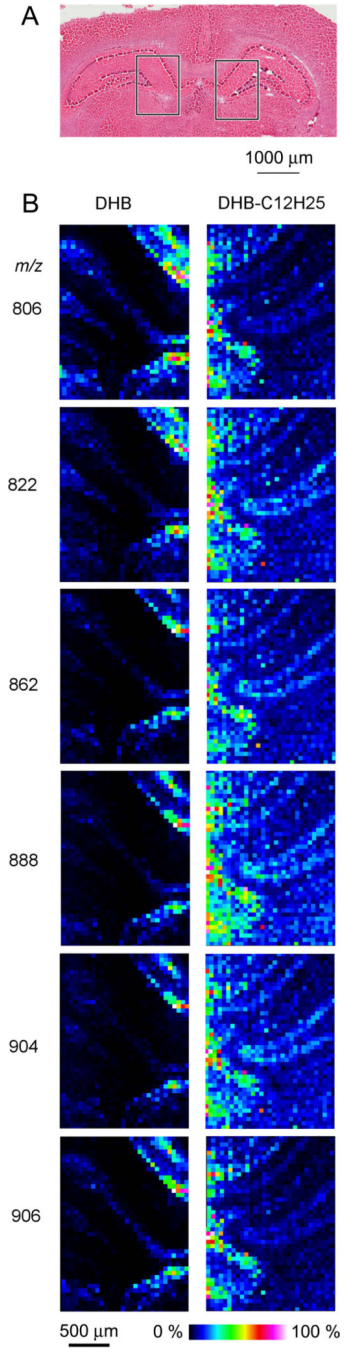

Figure 6. MALDI-MSI of brain slices with DHB and DHB-$C_{12}H_{25}$

A near-serial section (panel A) was stained with hematoxylin and eosin (H&E) and the locations for the MALDI-MSI analysis noted on the image (black rectangles). Tissue sections were prepared with DHB (left hemisphere) and DHB-$C_{12}H_{25}$ (right hemisphere) and analyzed by MALDI-MSI in negative ion mode (panel B). The lipid distribution in the Dentate Gyrus (DG) of the hippocampus was analyzed with a 50 µm raster. Representative pictures from three independent experiments are shown.

Table 1

Species of lipids detected in negative ion mode

Abbreviations: PI = phosphatidylinositol, PG = phosphatidylglycerol, ST = sulfatide, h = hydroxy fatty acid, d = dihydroxysphingosine. Chain assignments are given according to literature reports. Ion *m/z* values are given as the apex of the monoisotopic peak; the ion at *m/z* 834 is isobaric for two potential species.

m/z	Phospholipid or sphingolipid class	Fatty acid (number of carbon atoms : number of double bonds)	References
804.5	ST	d18:1/18:1	[34]
806.6	ST	d18:1/18:0	[34], [45]
822.6	ST	d18:1/h18:0	[34]
834.6	ST	d18:1/20:0	[45]
834.6	PS	18:0/22:6	[34]
850.7	ST	d18:1/h20:0	[34]
857.6	PI	16:0/20:4	[34]
860.7	ST	d18:1/22:1	[34]
862.7	ST	d18:1/22:0	[34], [45]
878.7	ST	d18:1/h22:0	[34], [45]
883.6	PI	18:1/20:4	[34]
885.6	PI	18:0/20:4	[34]
888.7	ST	d18:1/24:1	[34], [45]
890.7	ST	d18:1/24:0	[34], [45]
904.7	ST	d18:1/h24:1	[34], [45]
906.8	ST	d18:1/h24:0	[34], [45]
916.8	ST	d18:1/26:1	[34], [45]
918.7	ST	d18:1/h25:1	[45]
934.7	ST	d18:1/h26:0	[45]